


## Functional cargos of exosomes derived from Flk-1<sup>+</sup> vascular progenitors enable neurulation and ameliorate embryonic anomalies in diabetic pregnancy

Songying Cao<sup>1</sup>, Yanqing Wu<sup>1,4</sup>, E. Albert Reece<sup>1,2</sup>, Cheng Xu<sup>1</sup>, Wei-Bin Shen<sup>1</sup>, Sunjay Kaul<sup>1,3,5</sup> & Peixin Yang<sup>1,2</sup> 

Various types of progenitors initiate individual organ formation and their crosstalk orchestrates morphogenesis for the entire embryo. Here we show that progenitor inter-organ communication across embryonic organs occurs in normal development and is altered in embryos of diabetic pregnancy. Endoderm fibroblast growth factor 2 (FGF2) stimulates mesoderm Flk-1<sup>+</sup> vascular progenitors to produce exosomes containing the anti-stress protein Survivin. These exosomes act on neural stem cells of the neuroepithelium to facilitate neurulation by inhibiting cellular stress and apoptosis. Maternal diabetes causes Flk-1<sup>+</sup> progenitor dysfunction by suppressing FGF2 through DNA hypermethylation. Restoring endoderm FGF2 prevents diabetes-induced survivin reduction in Flk-1<sup>+</sup> progenitor exosomes. Transgenic *Survivin* expression in Flk-1<sup>+</sup> progenitors or *in utero* delivery of survivin-enriched exosomes restores cellular homeostasis and prevents diabetes-induced neural tube defects (NTDs), whereas inhibiting exosome production induces NTDs. Thus, functional inter-organ communication via Flk-1 exosomes is vital for neurulation and its disruption leads to embryonic anomalies.

<sup>1</sup>Department of Obstetrics, Gynecology & Reproductive Sciences, University of Maryland School of Medicine, Baltimore, MD, USA. <sup>2</sup>Department of Biochemistry & Molecular Biology, University of Maryland School of Medicine, Baltimore, MD, USA. <sup>3</sup>Department of Surgery, University of Maryland School of Medicine, Baltimore, MD, USA. <sup>4</sup>Present address: Institute of Life Sciences, Wenzhou University, Zhejiang Province, 325035 Wenzhou, China. <sup>5</sup>Present address: Division of Cardiovascular-Thoracic Surgery, Ann & Robert H. Lurie Children's Hospital of Chicago, 225 E. Chicago Avenue, Chicago, IL 60611, USA. ✉email: [pyang@som.umaryland.edu](mailto:pyang@som.umaryland.edu)

The US infant mortality rate, a basic measure of public health, is among the highest among developed countries, and birth defects are a major cause of infant mortality<sup>1</sup>. The development of a normal embryo and an eventual healthy newborn relies on temporal and spatial proliferation, differentiation, and migration of many organ-specific progenitors. Embryogenesis starts with a single totipotent zygote which is subsequently specified into three germ layer stem cells/progenitors and these progenitors further deduce to organ/tissue-specific progenitors. The expansion, differentiation, and function of these organ-specific progenitors instruct the processes of organogenesis leading to individual organ formation. Whereas the intrinsic function of progenitors in individual organ development has been extensively investigated, the crosstalk between progenitor across organs or tissues is less known.

Precise cell-to-cell communication across germ layers of the developing embryo is critical for normal embryogenesis. Soluble factors are conventional carriers for intercellular communication. However, exosomes, membrane-derived nanovesicles that mediate intercellular communication via functional cargos, may play important roles in embryonic development<sup>2</sup>. Functional exosome cargos include RNAs and proteins<sup>3</sup>. The survivin protein, an anti-stress, anti-apoptosis and pro-mitotic factor<sup>4</sup>, is present in the membrane of exosomes derived from cancer cells<sup>5</sup>. The deletion of the *Survivin* gene specifically in Flk-1<sup>+</sup> (vascular endothelial growth factor receptor 2 (VEGFR2) or Flk-1, hereafter referred to as Flk-1) progenitors, which first appear in the yolk sac mesoderm on mouse embryonic day 7 (E7)<sup>6</sup>, during embryonic organogenesis results in NTD formation<sup>7</sup>, suggesting that survivin produced by the Flk-1<sup>+</sup> progenitors can be packaged in exosomes and thus acts on neuroepithelial cells in promoting neurulation. Neuroepithelial cells engulf these exosomes, and the Survivin in these exosomes abrogates maternal diabetes-induced cellular stress and excessive neuroepithelial cell apoptosis, major etiological factors for NTD induction in diabetic pregnancy<sup>13</sup>. Testing these concepts is expected to clarify the role of Survivin in embryonic morphogenesis.

Neural tube defects (NTDs) are one of the leading causes of birth defects and are caused by many factors<sup>4</sup>, one of them being pregestational maternal diabetes, a major congenetic factor<sup>15</sup>. One of the keys to preventing NTDs is understanding how normal embryonic development occurs, thereby revealing potential in-points of dysregulation that lead to birth defects and potential therapeutic targets. Diabetic embryopathy can be used as a specific example in addressing how altered normal developmental processes lead to birth defect formation<sup>8</sup>. There are more than three million American and 60 million worldwide reproductive age women (18–44 years old) with diabetes, and these numbers will double by 2030. However, the mechanism underlying pregestational maternal diabetes-induced birth defects is unknown. Diabetic embryopathy is a devastating diabetic complication affecting both the mother and her fetus. Hyperglycemia, the excess of little sugar, is the major factor in mediating the teratogenicity of maternal diabetes, leading to NTD formation<sup>16–19</sup>.

Preexisting maternal diabetes disrupts the process of vasculogenesis<sup>20</sup>, which is initiated by the appearance of vascular endothelial growth factor receptor 2 (VEGFR2 or Flk-1, hereafter referred to as Flk-1)-positive hemangioblasts on mouse embryonic day 7 (E7) in the yolk sac mesoderm<sup>6</sup>. On E8 and later, maternal diabetes interrupts neurulation in the neuroectoderm, the innermost layer of the embryo, leading to neural tube defects (NTDs)<sup>11,21,22</sup>. Preliminary evidence suggests that there is crosstalk between components of early vasculopathy and those of late NTD formation, with the former being the proposed facilitators of the latter<sup>23,24</sup>. The spatial and temporal distinction between vasculogenesis and neurulation implies that maternal

diabetes affects intercellular communication among the three germ layers, thereby leading to diabetic embryopathy.

Survivin is implicated not only in development but also in the processes of carcinogenesis and aging<sup>4</sup>. How Survivin expression is regulated in Flk-1<sup>+</sup> progenitors may be very different than it is in cancer and aging cells. It has been shown that growth factor-responsive mitogen-activated protein kinase signaling activates *Survivin* transcription<sup>25</sup>, implicating growth factor regulation of Survivin expression during development. Indeed, maternal diabetes suppresses an array of vascular growth factors, including FGF2, leading to embryonic vasculopathy<sup>20,24,26</sup>. FGF2 derived from the endoderm acts on mesoderm Flk-1<sup>+</sup> progenitors to promote embryonic vasculogenesis<sup>27,28</sup>. Therefore, it is thought that the augmenting effect of FGF2 on Flk-1<sup>+</sup> progenitors transpires through the stimulation of *Survivin* transcription and subsequently enhances the production of Survivin-containing exosomes.

Maternal diabetes alters epigenetic modifications by increasing DNA methylation and suppressing histone acetylation during embryonic neurulation<sup>29–31</sup>. DNA hypermethylation accounts for the downregulation of neurulation essential genes in the neuroepithelium in diabetic pregnancy<sup>29</sup>. The mechanism underlying maternal diabetes-repressed vascular growth factor gene expression leading to embryonic vasculopathy is unknown. However, the green tea polyphenol epigallocatechin-3-gallate, which has a preventive effect on diabetic embryopathy through inhibition of DNA hypermethylation<sup>29</sup>, rescues embryonic vasculopathy in diabetic pregnancy<sup>32</sup>. This evidence supports the hypothesis that DNA hypermethylation represses FGF2 in diabetic embryopathy.

Here, we report exosomal regulation and communication across the yolk sac to the neuroepithelium in mediating the essential role of vascular Flk-1<sup>+</sup> progenitors in guiding neuroepithelial cells for ensured neurulation. FGF2 in the endoderm, restrained by DNA methylation, activates *Survivin* expression in Flk-1<sup>+</sup> progenitors, leading to the release of Survivin-contained exosomes. Neuroepithelial cells in the ectoderm internalize these Survivin-containing exosomes to ensure neurulation. Maternal diabetes suppresses FGF2 expression, leading to repression of *Survivin* and Survivin-containing exosomes, disrupting the flux of this exosomal communication and resulting in NTD formation.

## Results

### Maternal diabetes-induced DNA methylation inhibits FGF2 expression.

We hypothesized that molecular defects in the vascular progenitors of early vasculogenesis trigger the neuroepithelial cell dysfunction leading to NTD formation. To test this hypothesis, we examined the expression of fibroblast growth factor 2 (FGF2), which induces mesoderm epiblast cells to differentiate into Flk-1<sup>+</sup> progenitors in the mesoderm<sup>33,34</sup>. On E7.5, maternal diabetes reduced the abundance of *Fgf2* mRNA and protein (Fig. 1a, b). DNA hypermethylation typically occurs at CpG islands in the promoter regions of target genes to silence gene expression. A CpG island in the *Fgf2* gene promoter was identified (Fig. 1c), and methylation-specific PCR showed increased methylation in this CpG island (Fig. 1d). The methylated cytosine frequency of the 64 CpG sites in the CpG island of *Fgf2* was increased more than four-fold by maternal diabetes (Fig. 1e–f). Treatment with the DNA methylation inhibitor RG108<sup>35</sup> restored *Fgf2* promoter-driven luciferase activity suppressed by high glucose (Fig. 1g). These findings collectively support the hypothesis that the high glucose in maternal diabetes represses *Fgf2* expression in the endoderm through DNA hypermethylation.

### FGF2 restoration ameliorates embryonic vasculopathy in diabetic pregnancy.

To determine whether FGF2 reduction is

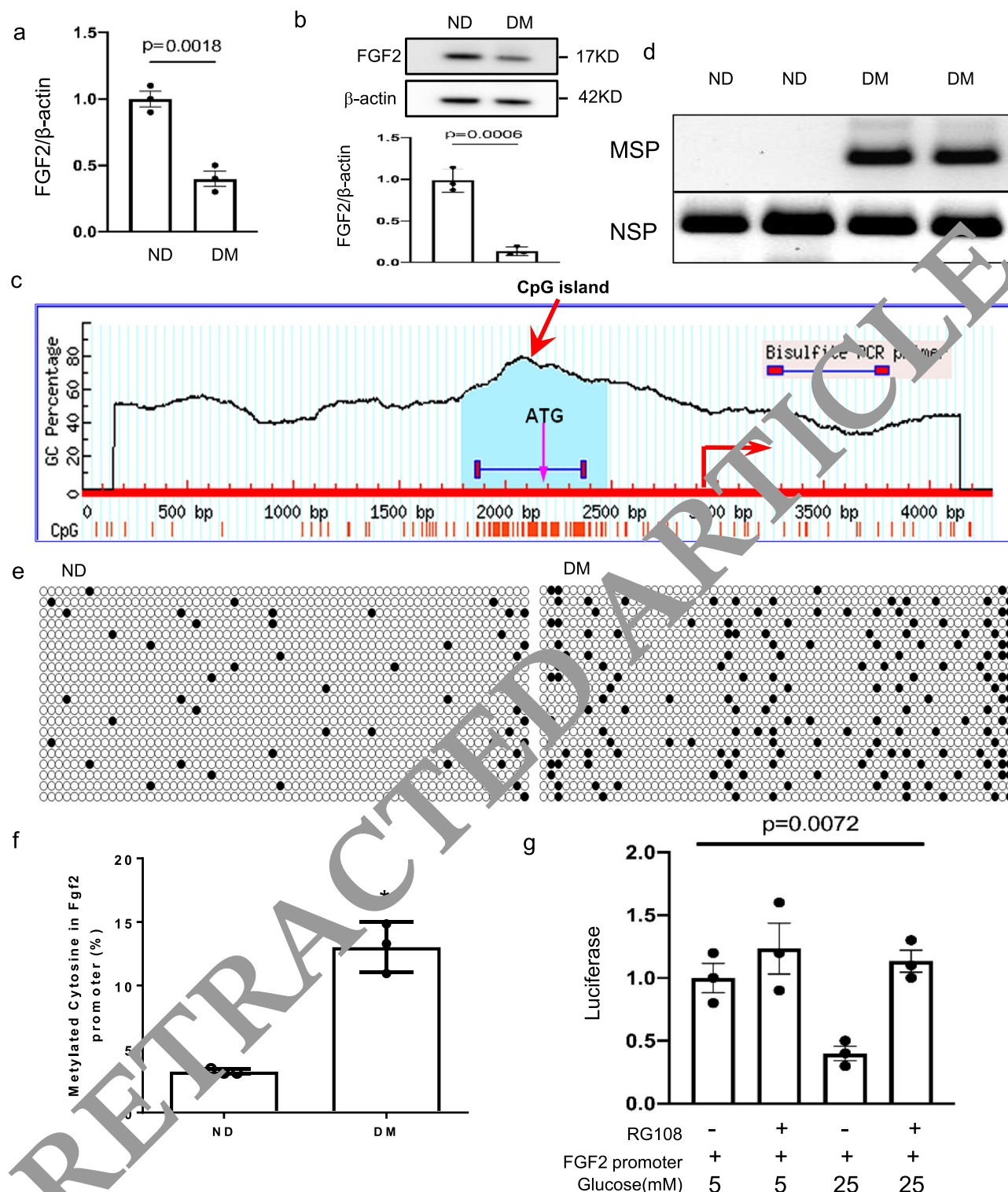
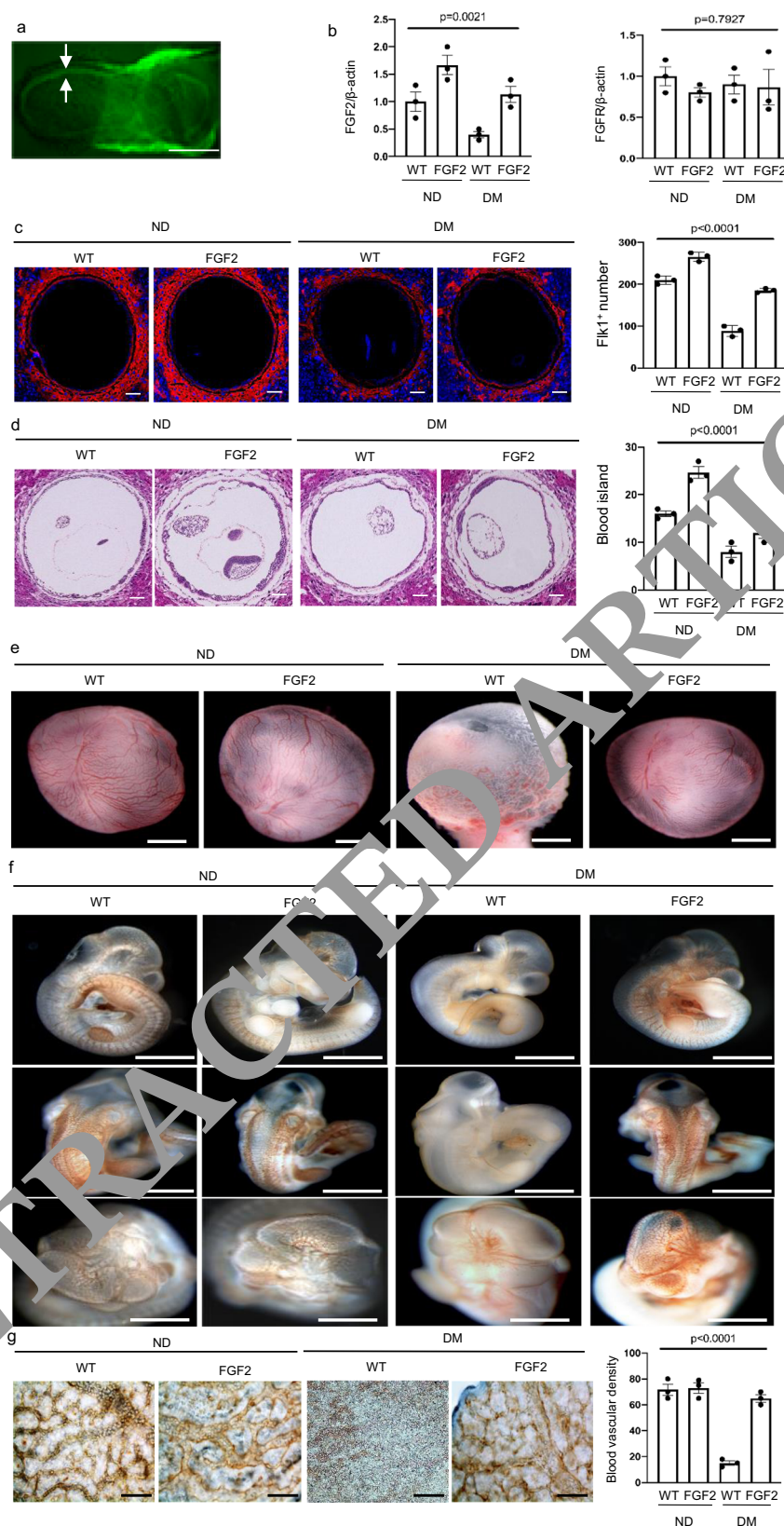


**Fig. 1 Maternal diabetes suppresses FGF2 expression through DNA hypermethylation.** **a**, **b** Abundance of FGF2 mRNA (**a**) and protein (**b**) in E7.5 conceptuses. **c** The CpG island (the light green area) of the *Fgf2* promoter in E7.5 conceptuses. **d** The degree of methylation in the CpG island of *Fgf2* promoter determined by Methylation-specific PCR (MSP) along with non-methylated specific PCR (NSP). **e** Methylated C (cytosine) frequencies in the 64 CpG sites of the CpG island after cloning CpG islands from the *Fgf2* promoter for bisulfite sequencing. DNA isolated from E7.5 embryos of three dams ( $n=3$ ) per group and DNA was cloned and sequenced twenty times per group. **f** Quantification of methylated cytosine from (**e**). **g** The methylation inhibitor RG108 restored *Fgf2* promoter luciferase reporter activity suppressed by high glucose (25 mM glucose) in the yolk sac endoderm PYS2 cell line. Cells experiments were repeated three times ( $n=3$ ). Experiments were performed using three embryos from three different dam per group ( $n=3$ ). \* indicates significant difference compared to other groups ( $P < 0.05$ ). ND: nondiabetic; DM: diabetes mellitus.



responsible for vasculopathy in diabetic pregnancy, we generated a transgenic (Tg) mouse line in which the *Fgf2* open reading frame and a separate nuclear GFP were driven by the promoter of the embryonic endoderm marker transthyretin (TTR) (Supplementary Fig. 1). TTR-driven transgene expression was evident in the endoderm on E5.75 and later. GFP

was evident in the endoderm of embryos on E8.0 (Fig. 2a). FGF2-expressing Tg embryos had slightly increased levels of *Fgf2* mRNA under nondiabetic conditions (Fig. 2b). *Fgf2* Tg expression restored *Fgf2* mRNA expression suppressed by maternal diabetes and did not affect FGFR expression (Fig. 2b).



**Fig. 2 FGF2 overexpression ameliorates maternal diabetes-induced vasculopathy.** **a** GFP was robustly expressed in the endoderm of E8.0 yolk sac. Bar = 100  $\mu$ m. **b** mRNA abundance of *Fgf2* and *Fgfr*. **c** Imaging and quantification of Flk-1<sup>+</sup> progenitors in the yolk sac of E8.5 conceptuses, cell nuclei were counterstained with DAPI. 5  $\mu$ m serial cross (vertical) sections of E8.5 conceptuses were stained by the Flk-1 antibody and the number of Flk-1<sup>+</sup> progenitors in each yolk sac was calculated. Bars = 100  $\mu$ m. **d** Imaging and quantification of blood island numbers in the yolk sac of E8.5 conceptuses (HE staining). Yolk sac blood islands were counted and expressed against the yolk sac circumference. Ten sections of each conceptus were used and the data were averaged. Five conceptuses from different pregnant dams in each group were used to determine the numbers of blood islands in yolk sacs. Bars = 100  $\mu$ m. **e** View of blood vessels in the yolk sac of E10.5 embryo. Bars = 250  $\mu$ m. **f** CD31 staining in E10.5 embryos showing disruptive blood vessel formation in embryos exposed to maternal diabetes. Bars = 250  $\mu$ m. **g** Blood vessel density determined by CD31 staining in the yolk sacs of E10.5 conceptuses. For blood vessel density analysis, CD31 staining signals were quantified in each yolk sac. Bars = 25  $\mu$ m. Experiments were performed using three embryos from three different dam per group ( $n = 3$ ). \* indicates significant difference compared to other groups ( $P < 0.05$ ). ND nondiabetic, DM diabetes mellitus, WT wild type, FGF2, FGF2 transgenic mice.

Maternal diabetes impacted the whole process of embryonic vasculogenesis. The total number of Flk-1<sup>+</sup> progenitors in the yolk sac of E8.5 conceptus was reduced by maternal diabetes (Fig. 2c). A key process during embryonic vasculogenesis is the formation of blood islands in the yolk sac by Flk-1<sup>+</sup> progenitors. Consistent with the reduced number of Flk-1<sup>+</sup> progenitors, blood island formation in the yolk sac of the E8.5 conceptus was decreased in conceptuses exposed to diabetes (Fig. 2d). The reversal of FGF2 reduction restored the number of Flk-1<sup>+</sup> progenitors and blood islands (Fig. 2b, c) and rescued vascular defects in the yolk sac and the embryo (Fig. 2e, f), thus preventing the reduction of blood vessel density in the yolk sac (Fig. 2g).

**FGF2 restoration inhibits ER stress and NTD formation.** *Fgf2* Tg expression effectively led to a reversal of maternal diabetes-suppressed FGF2 expression and FGF receptor phosphorylation (Fig. 3a). In addition, FGF2 overexpression restored key vascular signaling pathways impaired by maternal diabetes (Supplementary Fig. 2a–g). The reduced abundance of key vascular signaling intermediates p-AKT, p-VEGFR2 and BMP4 by maternal diabetes was recovered by FGF2 overexpression and reached the level of the nondiabetic controls (Supplementary Fig. 2a, b, d, e, and g). The increased abundance of VEGFR1, a negative regulator of embryonic vasculogenesis, was blunted in the FGF2-expressing Tg embryos (Supplementary Fig. 2c, e).

We next sought to determine whether correcting vascular defects via FGF2 would mitigate the diabetes-induced stress pathway in the neuroepithelium. Oxidative stress-induced endoplasmic reticulum (ER) stress that leads to apoptosis is manifested during failed neurulation during diabetic pregnancy<sup>9,36,37</sup>. Superoxide was abundant in the neuroepithelium of the WT embryos in diabetic dams but was diminished in the neuroepithelium of the WT embryos in nondiabetic dams and FGF2-expressing Tg embryos in nondiabetic and diabetic dams (Supplementary Fig. 3a). Maternal diabetes-induced increase in lipid peroxidation was also diminished in the FGF2-expressing Tg embryos (Supplementary Fig. 3b). The elevated abundance of the ER stress protein markers p-PERK, p-eIF2 $\alpha$ , IRE1 $\alpha$  and C/EBP homologous protein (CHOP) by maternal diabetes was abrogated in FGF2-expressing Tg embryos (Supplementary Fig. 3c–f). X-box binding protein 1 (XBP1) mRNA splicing, another indicator of ER stress, was induced by maternal diabetes and diminished in FGF2-expressing Tg embryos (Supplementary Fig. 3g). Furthermore, increased ER chaperone gene expression is also indicative of ER stress. The abundance of *Calnexin*, *GRP94*, *PDIA*, *BiP*, and *CHOP* mRNA was increased by maternal diabetes compared to levels in the WT embryos from nondiabetic dams and was abrogated by FGF2 overexpression (Supplementary Fig. 3h). Cleavage of the initiator caspase, caspase 8, and the executor caspase, caspase 3, was repressed by FGF2 overexpression under maternal diabetic conditions (Fig. 3b). Correspondingly, the number of apoptotic cells in the neuroepithelium of the WT embryos from diabetic dams was higher than

that in the WT embryos from nondiabetic dams and FGF2 overexpression inhibited maternal diabetes-induced apoptosis (Fig. 3c). These findings support the hypothesis that restoring FGF2 expression in the endoderm blocks maternal diabetes-induced cellular stress and apoptosis in the neuroepithelium.

To assess whether restoring FGF2 during vasculogenesis ameliorates maternal diabetes-induced NTDs, we examined NTD formation on E10.5. FGF2 overexpression did not affect embryonic development as indicated by the WT and FGF2-overexpressing E10.5 embryos being morphologically indistinguishable (Fig. 3d, Supplementary Table 1). Further analysis indicated a lower NTD incidence in the FGF2-expressing Tg embryos than in the WT counterparts that developed under diabetic conditions (Fig. 3d, Supplementary Table 1). We observed that 23.1% of the WT embryos in diabetic dams exhibited NTDs, which was higher than that of the WT embryos in nondiabetic dams (0%) (Fig. 3d, Supplementary Table 1), whereas only 5.7% of the FGF2-expressing Tg embryos (5.7%) exhibited NTDs (Fig. 3d, Supplementary Table 1).

**Survivin is the FGF2 target gene in Flk-1<sup>+</sup> progenitors.** Next, we sought to identify the target gene of FGF2 in the mesoderm. Deleting the gene *Survivin*, which encodes the inhibitor of apoptosis protein<sup>38</sup> in vascular endothelial progenitor cells, results in NTDs<sup>7</sup>. Survivin also combats cellular stress<sup>39</sup>. For these reasons, we proposed that Survivin is the FGF2 responsive gene in Flk-1<sup>+</sup> progenitors in the mesoderm. Restoring FGF2 expression reversed maternal diabetes-induced suppression of Survivin mRNA and protein expression in the developing embryo (Fig. 4a). In yolk sac endoderm PYS2 cells, FGF2 stimulated luciferase reporter activity driven by the *Survivin* promoter (Fig. 4b) and normalized Survivin mRNA and protein down-regulation induced by high glucose (Fig. 4c). FGF2 knockdown mimicked high glucose in repressing *Survivin* promoter activity (Fig. 4d) and in suppressing Survivin mRNA and protein expression (Fig. 4e).

**FGF2 abrogates the reduction in Survivin in the cargo of exosomes from Flk-1<sup>+</sup> progenitors.** Exosomes, small extracellular vesicles (50–150 nm), mediate cell-to-cell communication<sup>40</sup>. Survivin has been demonstrated to be incorporated as exosomal functional cargo<sup>5</sup>. High glucose did not affect the number of exosomes produced by a yolk sac cell line but decreased the abundance of Survivin in the exosomal cargo (Fig. 4f). FGF2 overexpression rescued Survivin expression in exosomal cargo that had been suppressed by high glucose (Fig. 4f). In contrast, FGF2 knockdown mimicked high glucose in that it reduced Survivin levels in the exosomal cargo but did not affect the cell production of exosomes (Fig. 4g). To determine the direct effect of high glucose on embryonic Flk-1<sup>+</sup> progenitors, we isolated Flk-1<sup>+</sup> progenitors on E8. High glucose suppressed Survivin expression in the exosomes

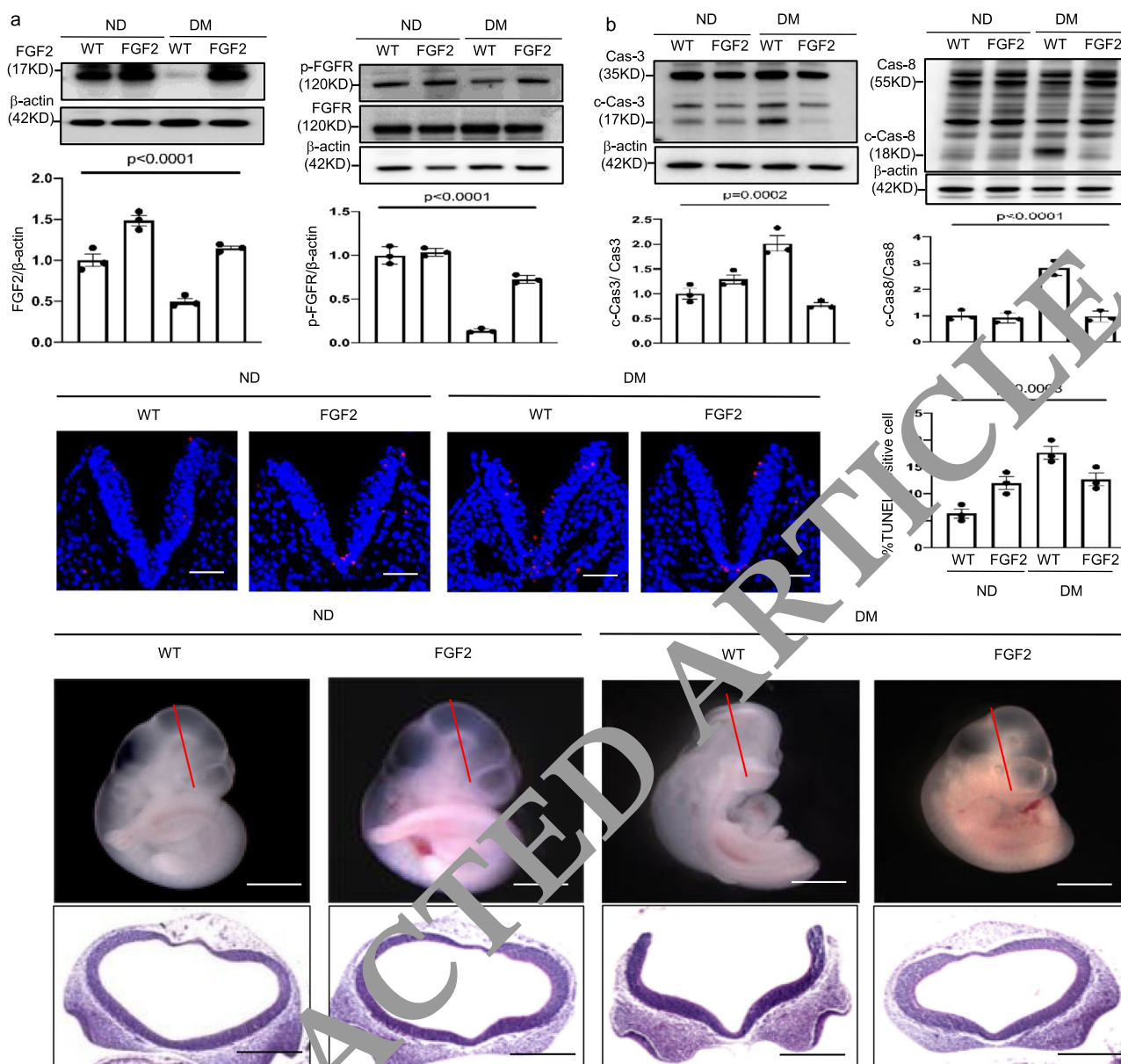


**Fig. 3 FGF2 overexpression alleviates maternal diabetes-induced apoptosis and NTD formation.** **a** Protein abundance of FGF2 and (p)-FGFR in E8.5 embryos. **b** Protein abundance of caspase 3 and caspase 8 in E8.5 embryos. **c** Representative TUNEL assay imaging showing apoptotic cells (red dots) in sections at the midbrain-hindbrain boundary of the E8.5 neuroepithelium. Cell nuclei were stained with DAPI (blue), bars = 30  $\mu$ m. The bar graph shows quantification of TUNEL-positive cells. **d** Imaging of WT and FGF2 Tg overexpressing embryos. Experiments were performed using three embryos from three different dams per group ( $n = 3$ ). Bars = 200  $\mu$ m and 100  $\mu$ m, for the top panel and the low panel, respectively. \* indicates significant difference compared to other groups ( $P < 0.05$ ). ND nondiabetic, DM diabetes mellitus, WT wild type, FGF2 FGF2 transgenic mice.

produced by isolated E8 Flk-1<sup>+</sup> progenitors, and FGF2 abolished this suppression (Fig. 4h). Survivin protein abundance was decreased in the exosomes derived from Flk-1<sup>+</sup> progenitors with FGF2 knockdown compared with the level in Flk-1<sup>+</sup> progenitors treated with control siRNA (Fig. 4i). FGF2 knockdown and high glucose did not affect the exosome production ability of cultured Flk-1<sup>+</sup> progenitors (Fig. 4i). These findings collectively suggest that FGF2 is essential for Survivin expression and its inclusion in the exosomal cargo of Flk-1<sup>+</sup> progenitors.

**Survivin restoration in Flk-1<sup>+</sup> progenitors ameliorates vasculopathy and prevents NTD formation.** To determine the role of Survivin reduction in diabetic embryopathy, we created a transgenic mouse line in which GFP (myc-tagged *Survivin*) was

specifically expressed in Flk-1<sup>+</sup> progenitors (Supplementary Fig. 4; Fig. 5a). *Survivin* transgenic overexpression restored Survivin expression that had been suppressed by maternal diabetes during vasculogenesis (Fig. 5b, c). We next aimed to reveal the cell-autonomous effect of Survivin by examining Flk-1<sup>+</sup> progenitor-initiated vasculogenesis. The total number of Flk-1<sup>+</sup> progenitors was reduced by maternal diabetes, and restoring Survivin expression in Flk-1<sup>+</sup> progenitors sustained their quantity under diabetic conditions (Fig. 5d), supporting a cell-autonomous effect of Survivin in Flk-1<sup>+</sup> progenitors. Blood island number and vessel density in Survivin-overexpressing conceptuses in diabetic dams reached a quantity similar to those in conceptuses in nondiabetic dams (Fig. 5e to h). Therefore, Survivin in Flk-1<sup>+</sup> progenitors exerts a dual functional role in embryonic development: a cell-autonomous effect in vasculogenesis and a paracrine effect on

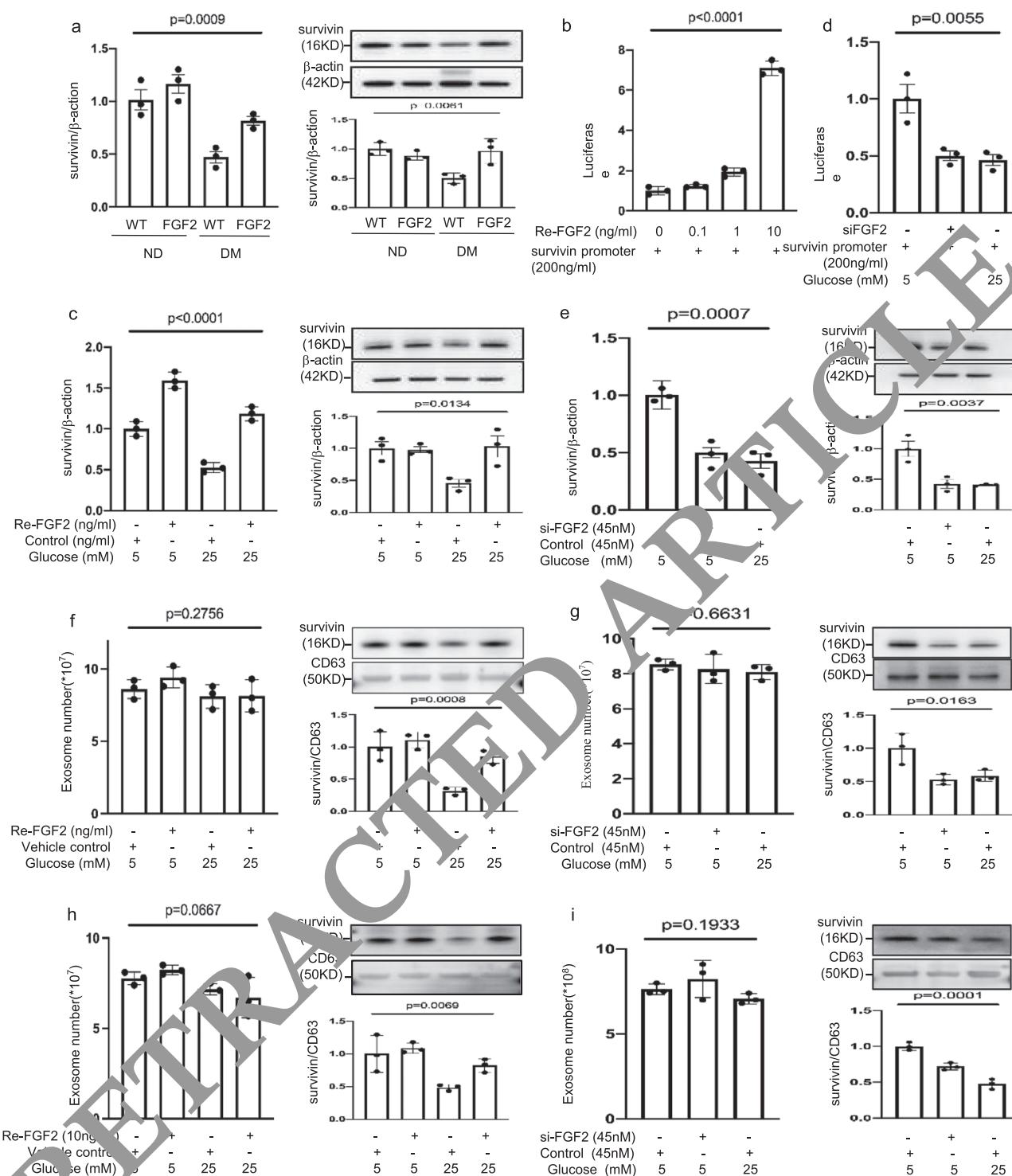


**Fig. 4 FGF2 induces Survivin expression and enriches Survivin in exosomes.** **a** Survivin mRNA and protein abundance in E8.5 wild type (WT) and FGF2 Tg embryos from nondiabetic or diabetic dams. **b** Luciferase reporter activity driven by the *Survivin* promoter. Re-FGF2: human recombinant FGF2. **c** Survivin mRNA and protein expression in normal glucose (NG; 5 mM glucose) and high glucose (HG; 25 mM glucose) culture conditions with Re-FGF2. **d** Luciferase reporter activity driven by the *Survivin* promoter. si-FGF2: siRNA FGF2. **e** Survivin mRNA and protein expression. **f, g** Exosome number and Survivin protein expression in exosomes treated by Re-FGF2 (**f**) or si-FGF2 (**g**). **h, i** Exosome number and Survivin protein expression in exosomes of isolated E8 Flk-1<sup>+</sup> progenitors treated by Re-FGF2 (**h**) or si-FGF2 (**i**). In (**f, h**), the vehicle control is water (equal volume of Re-FGF2 solution). Cell culture experiments were performed three times ( $n = 3$ ). Cells experiments were repeated three times ( $n = 3$ ). Experiments were performed using three embryos from three different dam per group ( $n = 3$ ). \* indicates significant difference ( $P < 0.05$ ) compared to other groups ( $P < 0.05$ ). ND nondiabetic, DM diabetes mellitus, WT wild type, FGF2 FGF2 transgenic mice.



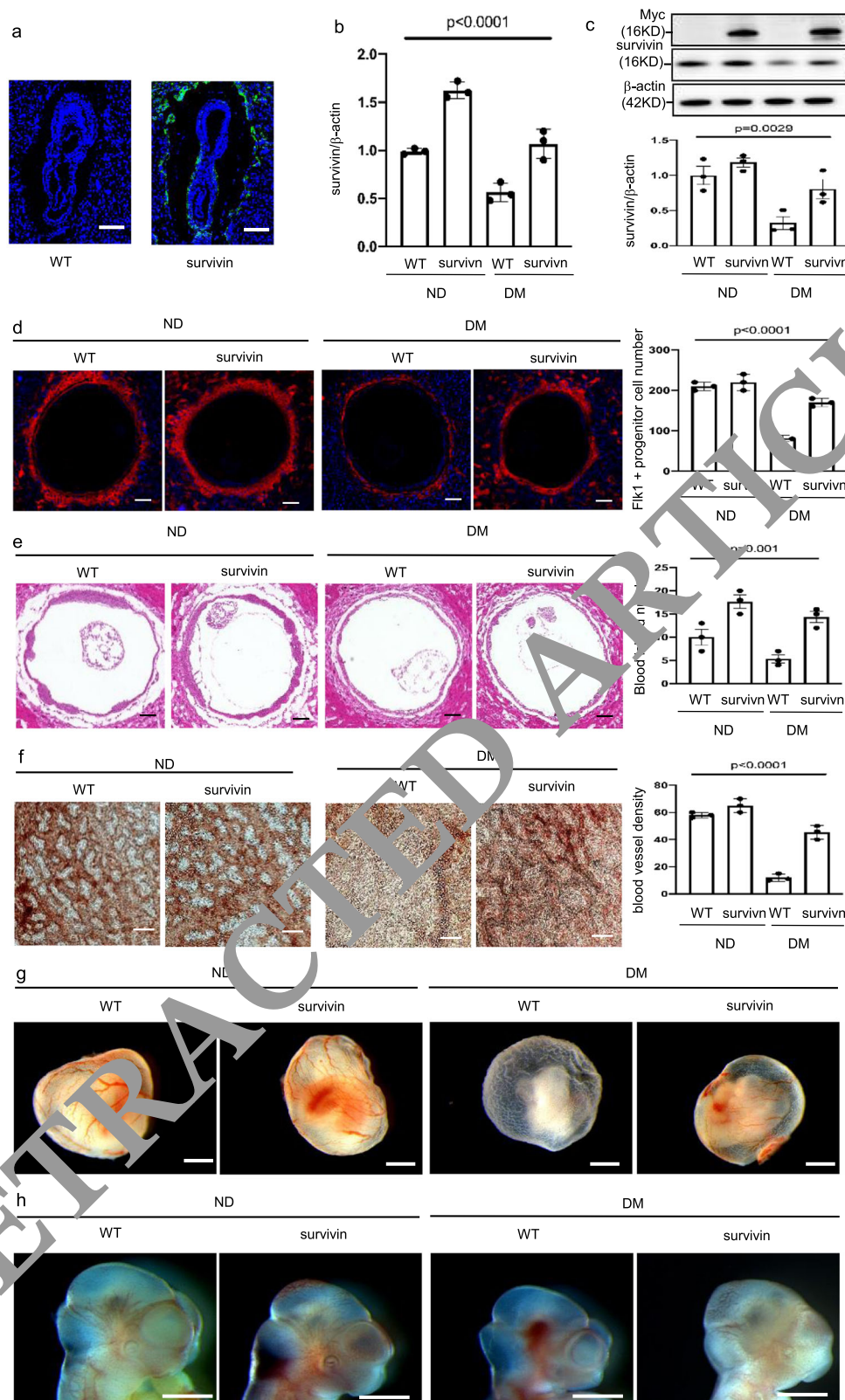


**Fig. 5 Survivin overexpression ameliorates maternal diabetes-induced vasculopathy.** **a** GFP was robustly expressed in Flk-1<sup>+</sup> progenitors in the yolk sacs of E8.5 conceptuses. Bars = 200  $\mu$ m. **b** Survivin mRNA and **c** protein expression in E8.5 embryos. **d** Imaging and quantification of Flk-1<sup>+</sup> progenitors in the yolk sacs of E8.5 conceptuses. Cell nuclei were stained with DAPI (blue). Bars = 100  $\mu$ m. **e** Imaging and quantification of blood island numbers in the yolk sacs of E8.5 conceptuses (HE staining). Bars = 100  $\mu$ m. **f** Blood vessel density determined by CD31 staining in the yolk sacs of E8.5 conceptuses. Bars = 25  $\mu$ m. **g** View of blood vessels in the yolk sacs of E8.5 conceptuses. Bars = 100  $\mu$ m. **h** CD31 staining in E8.5 embryos showing disruptive blood vessel formation in embryos exposed to maternal diabetes. Bars = 125  $\mu$ m. Experiments were performed using three embryos from three different dam per group ( $n = 3$ ). \* indicates significant difference compared to other groups ( $P < 0.05$ ). ND nondiabetic, DM diabetes mellitus, WT wild type, Survivin Survivin transgenic mice.



neurulation through the exosomal communication of Flk-1<sup>+</sup> progenitors in the mesoderm and neuroepithelial cells in the neuroectoderm.

Because ER stress is an important factor in the pathogenesis of NTDs in diabetic pregnancy<sup>11</sup>, we evaluated ER stress markers to address the effect of *Survivin* transgenic overexpression in Flk-1<sup>+</sup> progenitors on cellular stress in neuroepithelial cells. The increase in ER stress markers, phosphorylated PERK, eIF2 $\alpha$ , and IRE1 $\alpha$ , and total CHOP, induced by maternal diabetes, was diminished by *Survivin* transgenic overexpression in neurulation stage embryos (Supplementary Fig. 5a–d). ER stress was shown to lead to caspase 8-dependent apoptosis in the neuroepithelium<sup>36</sup>. The cleavage of caspase 3 and 8 was also abrogated by *Survivin* transgenic overexpression (Fig. 6a). Thus, under diabetic conditions, the number of apoptotic cells in the developing neuroepithelium was reduced to a number similar to that in the nondiabetic group (Fig. 6b). Finally, *Survivin* overexpression in the Flk-1<sup>+</sup> progenitors ameliorated maternal diabetes-induced NTDs on E10.5 (Fig. 6c, Supplementary Table 2).

**Survivin-containing exosomes derived from Flk-1<sup>+</sup> progenitors target neuroepithelial cells.** To further elucidate the role of exosomal communication involving *Survivin* in neurulation, we isolated Flk-1<sup>+</sup> progenitors from embryos on E8.0 and harvested exosomes produced by these cells (Fig. 7a). The exosomes derived from Flk-1<sup>+</sup> progenitors in *Survivin*-expressing Tg embryos had enriched levels of *Survivin* (Fig. 7b). The Flk-1<sup>+</sup> progenitor exosomes could be effectively internalized by cultured neural stem cells (Fig. 7c). The *myc*-tagged *Survivin* in the Tg conceptuses was found in the Flk-1<sup>+</sup> progenitors in the E8.0 yolk sac and in the neuroepithelial cells (or neural stem cells) along with the exosome marker CD63 (Supplementary Fig. 6a). Electron microscopy silver staining showed the presence of the exosome marker CD63 in the engulfed *myc*-tagged *Survivin* (Supplementary Fig. 6b), supporting the hypothesis that neuroepithelial cells take up *Survivin*-containing exosomes derived from Flk-1<sup>+</sup> progenitors.

**Intra-amniotic delivery of *Survivin*-containing exosomes inhibits NTD formation.** The functional significance of *Survivin*-containing exosomes derived from E8.0 Flk-1<sup>+</sup> progenitors was also demonstrated by the intra-amniotic delivery of these exosomes to neurulation stage embryos on E8.0. The *Survivin*-containing exosomes were specifically internalized by the neuroepithelium (Fig. 7d), restored embryonic *Survivin* expression (Fig. 7e), inhibited ER stress (Fig. 7f), and blocked caspase 3 and 8 cleavage and neuroepithelial cell apoptosis under diabetic conditions (Fig. 7f, g). However, exosomes from neural stem cells did not efficiently target neural stem cells (Fig. 7c), did not restore *Survivin* expression (Fig. 7e), could not block ER stress (Supplementary Fig. 7), and did not inhibit caspase activation and apoptosis (Fig. 7f, g). Thus, *Survivin*-containing exosomes derived from Flk-1<sup>+</sup> progenitors reduced maternal diabetes-induced NTDs (Fig. 7h, Supplementary Table 3). In contrast, delivery of exosomes derived from neural stem cells without *Survivin* enrichment had no inhibitory effect on NTD formation in diabetic pregnancy (Fig. 7h).

**An exosome inhibitor mimics maternal diabetes by inducing NTDs.** To determine whether exosomes are essential for neurulation, we injected the exosome inhibitor GW4869<sup>41</sup> into dams from E7.0 to E8.5. Maternally injected GW4869 reached the embryo as indicated by GW4869 detection in the embryo (Fig. 7i). GW4869 inhibited exosome production in the developing embryos (Fig. 7i, j) and mimicked the teratogenic effect of

maternal diabetes on NTD induction (Fig. 7k, m, Supplementary Table 4). Exosome inhibition by GW4869 triggered ER stress in neurulation stage embryos and neuroepithelial cell apoptosis (Supplementary Fig. 8a–f), key cellular events leading to failed neurulation.

Thus, we revealed previously unappreciated crosstalk between the Flk-1<sup>+</sup> progenitors and neuroepithelial cells and *Survivin*-containing exosomes produced by Flk-1<sup>+</sup> progenitors mediate this crosstalk (Fig. 7n). The functional exosomal cargo *Survivin* is transcriptionally regulated by FGF2, which itself is controlled by DNA methylation (Fig. 7n). Deviation of this crosstalk via *fgf2* promoter hypermethylation leads to NTDs in diabetic pregnancy (Fig. 7n).

## Discussion

In the present study, we report crosstalk among components of the endoderm, mesoderm, and neuroectoderm via the growth factor FGF2 and the vascular progenitor-specific factor *Survivin*-containing exosomes. This crosstalk is essential for successful neurulation. Maternal diabetes disrupts this crosstalk by suppressing FGF2 expression in the endoderm and FGF2 reduction leads to the inhibition of *Survivin* expression in the Flk-1<sup>+</sup> vascular progenitor of the mesoderm. In diabetic pregnancy, the exosomes derived from Flk-1<sup>+</sup> progenitors, which contain less *Survivin*, cannot propel neural tube closure, leading to NTD formation. These findings reveal an innovative role for the *Survivin*-containing exosomes produced by Flk-1<sup>+</sup> progenitors in neurulation and indicates that the endoderm factor FGF2 sustains *Survivin* expression, a process is compromised by maternal diabetes.

DNA methylation is a process by which a methyl group is added at the C5 position of a cytosine to form 5-methylcytosine. DNA hypermethylation is an epigenetic modification leading to the suppression of gene expression. Once a CpG island enriched with CpG dinucleotides is hypermethylated, particularly in the promoter region of an active gene, the expression of the gene is suppressed. The current study revealed that FGF2 expression was suppressed by maternal diabetes due to hypermethylation of the CpG island residing in the *Fgf2* promoter. This finding is consistent with a previous finding showing that maternal diabetes increases DNA methylation of the CpG islands in neural tube closure-essential genes, leading to the suppressed expression of these genes<sup>29</sup>. It is not entirely clear how maternal diabetes induces DNA hypermethylation. Previous evidence suggests that maternal diabetes-induced oxidative stress is critical for this increase in DNA methylation because an antioxidant effectively inhibits maternal diabetes-induced DNA methyltransferase expression and subsequent DNA hypermethylation<sup>29</sup>. The current study makes clear that FGF2 is inhibited by DNA hypermethylation; however, the effect of maternal diabetes-induced DNA hypermethylation on the endoderm may be much broader than FGF2 repression. Other endoderm factors may also be affected and contribute to maternal diabetes-induced vasculopathy in the early conceptus.

A group of growth factors including FGF2 plays important roles in embryonic vasculogenesis; however, their contribution to other important developmental processes including neurulation has not yet been revealed. FGF2 exerts both autocrine and paracrine functions during embryonic development. In amphibians, FGF2 induces mesoderm formation<sup>28</sup>. FGF2 induces the differentiation of mesoderm epiblasts into Flk-1<sup>+</sup> progenitors<sup>33,34</sup>. FGF2 also acts on vascular progenitors by facilitating vascular morphogenesis in the mouse embryo<sup>27</sup>. The current study further reveals the effect of FGF2 on Flk-1<sup>+</sup> progenitors by demonstrating that FGF2 stimulates *Survivin*

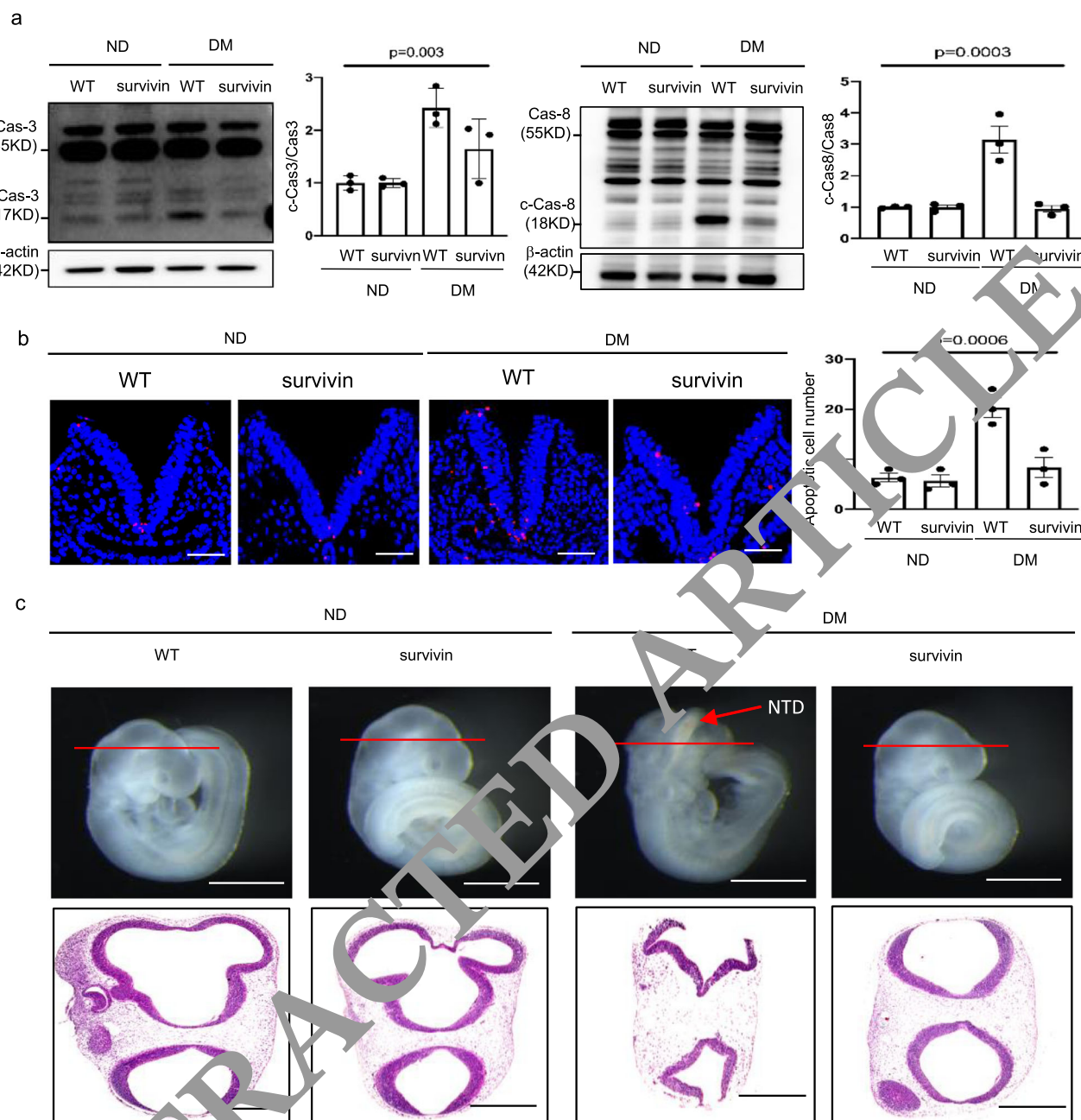
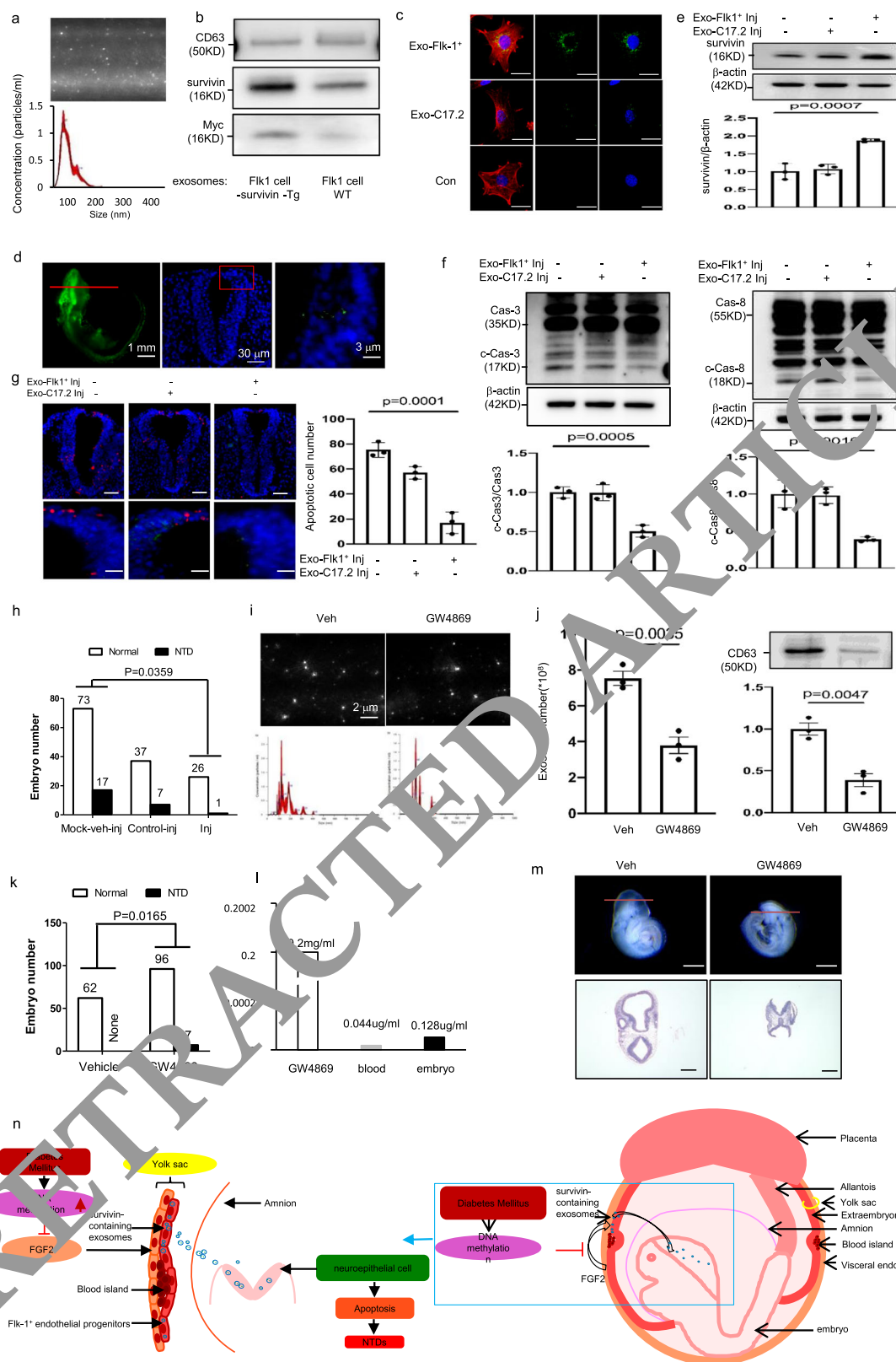


**Fig. 6 Restoring Survivin expression in Flk-1<sup>+</sup> progenitors reduces diabetes-induced apoptosis and NTD formation.** **a** Protein levels of cleaved caspase 3 and caspase 8 in E8.5 embryos. **b** Representative TUNEL assay imaging showing apoptotic cells (red dots) in the E8.5 neuroepithelium and quantification of TUNEL-positive cell numbers in the bar graph. Cell nuclei were stained with DAPI (blue), bars = 30  $\mu$ m. **c** Representative imaging of WT and Survivin transgenic overexpressing embryos showing an NTD embryo with an open neural tube. Bars = 200  $\mu$ m and 100  $\mu$ m, for the top panel and the low panel, respectively. Experiments were performed using three embryos from three different dams per group ( $n=3$ ). \* indicates significant difference compared to other groups ( $P<0.05$ ). ND nondiabetic, DM diabetes mellitus, WT wild type, Survivin Survivin transgenic overexpressing embryos.

expression in the Flk-1<sup>+</sup> progenitors, leading to the release of Survivin-enriched exosomes. Our results indicate that the alteration of this FGF2 function contributes to maternal diabetes-induced embryonic anomalies. The restoration of FGF2 expression in the endoderm via *Fgf2* Tg mice ameliorates maternal diabetes-induced vasculopathy and NTD formation. This beneficial effect of restored FGF2 expression depends on the rescue of Survivin expression in Flk-1<sup>+</sup> progenitors. The current study demonstrates that Survivin is a target gene of the FGF2 signaling. It cannot rule out the possibility that other genes are also FGF2 target genes in Flk-1<sup>+</sup> progenitors. The FGF-FGFR signaling may be redundant and compensatory during organogenesis because

*Fgf2* gene deletion in the mouse does not affect embryonic vasculogenesis<sup>42</sup>. Therefore, it is possible that under maternal diabetic conditions, multiple FGF ligands or even other endoderm growth factors are also severely suppressed by exposure to maternal diabetes. Nevertheless, restoring FGF2 can only mitigate maternal diabetes-induced embryonic defects, underscoring the critical contribution of FGF2 reduction to the induction of diabetic embryopathy.

In addition to soluble factor-mediated intercellular communications, other forms of intercellular communications have not been extensively studied during embryonic development. Exosomes enable cell-to-cell communication in spatially distinct



tissues or organs. Indeed, exosomes derived from Flk-1<sup>+</sup> progenitors, which exclusively reside in the yolk sac in early embryonic development, cross the intra-amniotic space to target cells in the neuroepithelium, which is in the innermost layer of the embryo. This may explain why the Flk-1<sup>+</sup> progenitor-specific

factor Survivin plays a critical role in neurulation. It has been shown that deletion of the *Survivin* gene specifically in endothelial progenitors results in NTD formation<sup>7</sup>. Survivin is effectively packaged into Flk-1<sup>+</sup> progenitor exosomes, and these Survivin-enriched exosomes are internalized by neuroepithelial



**Fig. 7 Survivin-enriched exosomes derived from Flk-1<sup>+</sup> progenitors prevent diabetic embryopathy and the exosome inhibitor induces NTDs.**

**a** Exosomes (Exo) derived from Flk-1<sup>+</sup> progenitors of E8.5 embryos. Exosomes (bright round dots) were directly detected by the NanoSight (#NS300, Malvern Panalytical). **b** Survivin protein expression in Flk-1<sup>+</sup> progenitor exosomes from Survivin transgenic (Tg) and Wild-Type (WT) E8.5 embryos. **c** Labeled exosomes (green) from Flk-1<sup>+</sup> progenitors but not C17.2 neural stem cells were up-taken by C17.2 neural stem cells labeled by nestin staining (Red). Cell nuclei were stained with DAPI (blue). Bars = 15  $\mu$ m. **d** Flk-1<sup>+</sup> progenitor exosomes (green) via in utero amniotic microinjections were specifically up-taken by neuroepithelial cells of E8.0 embryos. **e–g** Survivin protein (**e**), cleaved caspase 8 and caspase 3 (**f**) and TUNEL-positive apoptotic cells (**g**) after 36 h exosome microinjections into E8.0 embryos. Bars = 30  $\mu$ m and 1  $\mu$ m, for the top panel and the low panel, respectively. **h** Numbers of normal and NTD embryos after exosome injections. Mock: mock vehicle (Veh) injections. n was indicated in Table S3. **i, j** Exosome profile (**i**), exosome numbers and CD63 expression (**j**) in E8.5 embryos after the exosome inhibitor GW4869 injections. **k** Numbers of normal and NTD embryos after exosome injections (**L**) one-time measurement of GW4869 concentrations in E8.5 embryos. **m** Morphology of embryos. Bars = 100  $\mu$ m and 50  $\mu$ m, for the top panel and the low panel, respectively. **n** is a schematic diagram depicting the communication of Survivin-containing exosomes across germ layers, regulated by DNA hypermethylation of FGF2. Cells experiments were repeated three times ( $n = 3$ ). Experiments were performed using three embryos from three different dam per group ( $n = 3$ ). \* indicates significant difference compared to other groups ( $P < 0.05$ ). ND nondiabetic, DM diabetes mellitus, W wild type, Veh vehicle.

cells. Thus, Survivin-enriched exosomes facilitate communication between Flk-1<sup>+</sup> progenitors and the neuroepithelium and ensure the completion of proper neural tube closure.

Survivin, a member of the inhibitor of apoptosis (IAP) family proteins, not only inhibits cell death but also promotes cell proliferation<sup>4</sup>. It is upregulated in virtually all cancer cells and aged cells and thus has received much attention for cancer therapy<sup>38</sup>. During embryonic development, Survivin is predominantly expressed in Flk-1<sup>+</sup> progenitors and is essential for neurulation<sup>7</sup>. Survivin lacks intrinsic catalytic activity and thus functionally depends on its interactive partners<sup>4</sup>. Survivin blocks apoptosis through its interaction with other IAP proteins, inhibiting the caspase activation that initiates cell apoptosis<sup>4</sup>. Because caspase activation is critically involved in maternal diabetes-induced NTDs<sup>8,43</sup>, transgenic Survivin overexpression ameliorated NTDs in diabetic pregnancy, possibly through the suppression of caspase activation. Furthermore, Survivin abrogated the ER stress induced by maternal diabetes, which may also have been mediated by its binding partners. Survivin is present on the surface of exosomes derived from cancer cells<sup>5</sup>. While exosomes derived from Flk-1<sup>+</sup> progenitors contained abundant Survivin, the exact location of Survivin in these exosomes was not determined. Nevertheless, neuroepithelial cells that take up Flk-1<sup>+</sup> progenitor exosomes showed Survivin expression. FGF2 overexpression in the endoderm restored Survivin expression suppressed by maternal diabetes in Flk-1<sup>+</sup> progenitors. The stimulating effect of FGF2 on Survivin expression may rely on the activation of mitogen-activated protein kinase signaling, which has been shown to activate Survivin transcription<sup>25</sup>. Survivin can also be negatively regulated by two transcription factors, Forkhead box O3a (FoxO3a)<sup>44</sup> and p53<sup>45</sup>. The increased activity of these two transcription factors is pivotal to the induction of diabetic embryopathy<sup>8,46,47</sup>. The regulatory network for Survivin expression in Flk-1<sup>+</sup> progenitors needs to be further determined. However, it is clear that Survivin is a Flk-1<sup>+</sup> progenitor factor and a central player in neurulation by acting on neuroepithelial cells through exosome communication and Survivin regulation profoundly mediates the teratogenicity of maternal diabetes, leading to NTD formation.

Exosomal intercellular communication clearly shows specificity. Neural stem cells cannot effectively take up exosomes derived from themselves. On the other hand, Flk-1<sup>+</sup> progenitor exosomes are effectively internalized by neural stem cells or neuroepithelial cells. When Flk-1<sup>+</sup> progenitor exosomes are delivered to the inside of the amniotic sac, these exosomes specifically enter neuroepithelial cells and reduce NTD formation in diabetic pregnancy. Thus, Flk-1<sup>+</sup> exosomes specifically target neuroepithelial cells of the developing embryo and can be used for the delivery of genes and other functional cargos into these cells. Because exosomes are noncytotoxic, have low

immunogenicity, and are easy to store, and have a long lifespan and high cargo loading capacity, they have been proposed to be nanometric vehicles for therapeutic agent and gene delivery<sup>48</sup>. The mechanism underlying exosome-specific targeting is still unclear. One potential mechanism involves membrane receptors on the exosomes, which bind cell surface proteins of the recipient cells<sup>49</sup>. The surface molecular contents of Flk-1<sup>+</sup> progenitor exosomes need to be further characterized to understand their specific targeting to neuroepithelial cells.

During embryonic development, the vasculature is the first system to develop. Maternal diabetes adversely impacts embryonic vasculogenesis leading to yolk sac vasculopathy in the mouse embryo<sup>20,24,50</sup>. Vasculopathy in diabetic pregnancy is caused by alterations to a group of vascular growth factors that are essential for embryonic vasculogenesis<sup>50</sup>. Among these growth factors, FGF2 downregulation in the endoderm appears to be the most important factor for the induction of vasculopathy in diabetic embryopathy. Previous studies have suggested a possible connection between early vasculopathy in the yolk sac and late-forming structural birth defects<sup>23,24</sup>. Because either restoration of FGF2 or Survivin in the mesoderm Flk-1<sup>+</sup> progenitors ameliorates both vasculopathy and NTDs in diabetic pregnancy, the present study establishes a possible causal relationship between early vasculopathy in the yolk sac and late NTD formation. Using the currently available technologies, we have provided strong evidence that Survivin is a functional exosomal cargo and is present in the developing neuroepithelium. The delivery of Survivin-contained exosomes into the amniotic sac reduces NTD incidence in diabetic embryopathy. Electronic microscope examination reveals exosome-enclosed Survivin protein in neuroepithelial cells. However, this evidence cannot completely exclude the positive effect of restored yolk sac vasculature by Survivin on neurulation.

The NTD rates in this study are in line with published studies from us and others<sup>10,11,51–56</sup>. In human, maternal diabetes does not induce 100% of birth defects<sup>15</sup>. Maternal diabetes-induced cellular stress levels need reach a threshold that leads to the formation of a birth defect<sup>57</sup>. Clinical studies have demonstrated that hyperglycemia levels of maternal diabetes are positively associated with the incidence of birth defects<sup>16</sup>. In an in vitro animal embryo culture study demonstrates that at the level of 750 mg/dl glucose, all embryos are defective<sup>58</sup>. Such level of hyperglycemia is unrealistic in human conditions. The hyperglycemia level between 350 and 450 mg/dl in our mouse model of diabetic embryopathy is in the range of the hyperglycemia levels in pregnant women with pregestational maternal diabetes<sup>16,59</sup>. Thus, our model faithfully reflects the human conditions. Likewise, the dose of the exosome inhibitor is at a relatively low level to avoid any adverse maternal outcome. Higher level of the

exosome inhibitor could lead to higher NTD incidence. Nevertheless, the exosome inhibitor study shows that exosome production is critical for neurulation.

Our findings reveal a mechanism underlying maternal diabetes-induced NTDs. During embryogenesis, proper communication among the three germ layers through exosomes is required for vasculogenesis and neurulation. The growth factor FGF2, produced by the endoderm, exerts its effect on Flk-1<sup>+</sup> progenitors in the mesoderm, leading to the release of Survivin-enriched exosomes. These exosomes act on the neuroectoderm to prevent cellular stress and neuroepithelial cell apoptosis. Blocking this pathway under maternal diabetic conditions results in vasculopathy, which, in turn, contributes to NTD formation. Therefore, our study uncovers the importance of exosomes in diabetic embryopathy and the relationship between vasculogenesis and neurulation during early embryonic development.

## Methods

**Animals and reagents.** The procedures for animal use were approved by the University of Maryland School of Medicine Institutional Animal Care and Use Committee. Wild-type (WT) C57BL/6 J mice were purchased from the Jackson Laboratory (Bar Harbor, ME). The DNA construct for the FGF2 transgenic mice (FGF2-Tg) was derived from the pTTR1ExV3 vector provided by Dr. Terry A. Van Dyke (Department of Biological Sciences, University of Pittsburgh, PA). The vector contains 3 kb transthyretin (TTR) promoter, its exon 1, intron 1, and exon2 fused with the SV40 polyA. We cloned the FGF2 open reading frame (ORF) followed by an IRES site and a nuclear specific expressing GFP (Clontech, Mountain View, CA94043) in exon 1. After oocyte injection, 6 founders carried the FGF2 transgene, 3 of them showed GFP expression and one line (#134) was selected for experiment. The DNA construct for the *Survivin* transgenic mice was driven by the Flk-1 promoter, which was cloned based on a previous report<sup>60</sup>. The mouse Flk-1 promoter fragment (−640 bp ~ +299 bp, the Transcriptional Start Site was defined as +1) was amplified by PCR, and then was inserted into 5' of the *Survivin* ORF (Cat#: MR223428, Origene, Rockville, MD 20850). An IRES site and a nuclear specific expressing GFP were added to the 3' of the *Survivin* ORF. An intronic fragment with the 3' region of the first intron (+1677 bp ~ +3947 bp) of the Flk-1 gene was PCR cloned and ligated to the 3' of GFP. There were 15 founders that carried the *Survivin* transgene, and one was selected for our experiment.

All Tg animal lines were generated in the Genome Modification Facility at Harvard University using the C57BL/6J background as previously described<sup>11</sup>. Streptozotocin (STZ; Sigma (St. Louis, MO) was dissolved in sterile 0.1 M citrate buffer (pH 4.5).

**Mouse models of diabetic embryopathy.** Our mouse model of diabetic embryopathy has been described previously<sup>8,10,36,61,62</sup>. Briefly, 10-week-old female mice were intravenously injected daily with 75 mg/kg STZ over two days to induce diabetes. Diabetes was defined as 12 h fasting blood glucose level of  $\geq 250$  mg/dL. Male and female mice were paired at 3:00 P.M. and 1 day (D1) (E0.5) of pregnancy was established by the presence of the vaginal plug at 8:00 A.M. the next morning. Female mice injected with vehicle served as the non-diabetic controls. On E7.5, E8.5, E9.5, or E10.5 mice were euthanized and embryos were dissected out of the uteri for biochemical and molecular analysis. The exosome inhibitor GW4869 (Sigma, St. Louis, MO) was injected daily in nondiabetic pregnant dams from E7.0 to E8.0. NTDs were examined at E10.5.

**Cell culture and transfection.** The C17.2 mouse neural stem cell line the European Collection of Cell Culture (Salisbury, UK), and the yolk sac endoderm PYS2 cell line (ATCC® CRL-2745™) were maintained in DMEM (5 mM glucose) supplemented with 10% FBS, 100 U/ml penicillin, and 100 mg/mL streptomycin at 37 °C in a humidified atmosphere of 5% CO<sub>2</sub>. Mouse recombinant FGF2 (#3139-FB; R&D Systems, Minneapolis, MN) was used at a final concentration of 10 ng/ml. Lipofectamine 2000 (Invitrogen, Carlsbad, CA) was used according to the manufacturer's protocol for transfection of siFGF2 and control siRNA (Invitrogen, Carlsbad, CA) into the cells. After seeding for 12 h, cells were transfected with recombinant FGF2 and cultured in 1% FBS for 8 h, after which cells were cultured in 10% FBS and collected after 48 h for analysis.

**Isolation of Flk-1<sup>+</sup> endothelial progenitor cells.** Flk-1<sup>+</sup> progenitor cells were isolated from the E8 yolk sac. Yolk sacs were minced in phosphate-buffered saline PBS (Thermo Fisher Scientific, Waltham, MA), digested with 1 mg/ml of collagenase type I (Sigma, St. Louis, MO) and incubated on an orbital shaker at 37 °C for 30–45 min. Following the collagenase treatment, cells were washed twice with growth medium [EBM-2, fetal bovine serum (10%), hFGF-basic (0.5 ml), hydrocortisone (0.2 ml), VEGF (0.5 ml), IGF-1 (0.5 ml), ascorbic acid (0.5 ml), hEGF (0.5 ml), GA-100 (0.5 ml)] before being plated. Cells were trypsinized (Lonza,

Walkersville, MD) and sorted for Flk-1 with MACS microbeads (Miltenyi Biotec, Bergisch Gladbach, Germany) as per the kit instructions. The Flk-1<sup>+</sup> progenitor cells were collected and cultured in growth medium as mentioned above.

**Immunofluorescent staining.** Tissue sections were fixed with 4% paraformaldehyde (pH7.4) for 30 min at room temperature, followed by permeabilization with 0.25% Triton-X100 (Sigma, St. Louis, MO) for 10 min. Samples were blocked for 30 min in PBS with 10% donkey serum and incubated with CD63 (Santa Cruz Biotechnology, Dallas, TX), Nestin (1:1000, Invitrogen, Carlsbad, CA), Flk-1 (1:200, Santa Cruz Biotechnology, Dallas, TX) and Myc-tag antibodies (1:200, Cell Signaling Technology, Danvers, MA) overnight at 4 °C. After washing three times with PBS, samples were incubated with Alexa Fluor 488 or 594-conjugated secondary antibody (1:1000, Invitrogen, Carlsbad, CA) for 2 h, followed by DAPI (Invitrogen, Carlsbad, CA) cell nuclear counterstaining for 10 min, then mounted with aqueous mounting medium (Sigma, St. Louis, MO). Confocal immunofluorescent images were recorded by a laser scanning microscope (LSM 710 META; Zeiss, Germany).

**Exosome extraction and labeling.** Cells and debris were removed from cell culture media via centrifugation at 2000 × g for 30 min at 4 °C. Supernatants containing the cell-free culture media were transferred to a new tube without disturbing the pellet. Total Exosome Isolation (#4478359, Invitrogen, Carlsbad, CA) at 0.5 volume of the collected supernatants was added to each tube. The cell culture media/reagent mixture was mixed well by vortex and pipetting up and down until it became a homogeneous solution, and then was incubated at 4 °C overnight. After incubation, the samples were centrifuged at 10,000 × g for 1 h at 4 °C and the supernatants were discarded. Exosomes were contained in the pellet at the bottom of the tube (not visible in most cases). The pellet was re-suspended in 1 ml of 1 X PBS and 100 µg/ml RNase300 (Malvern Panalytical) was used to measure the exosomes. The presence of exosomes was confirmed by Western blot using the external marker CD63 (Santa Cruz Biotechnology, Dallas, TX). Exosomes were suspended in 1 ml Diluent C (Sigma, St. Louis, MO) and labeled by incubating with Cy3-labeled fluorescent dye (Sigma, St. Louis, MO) for 5 min in the dark at room temperature. An equal volume of 1% BSA in PBS was added to each tube to stop the staining, with an additional incubation period of 1 min to allow binding of excess dye. The labeled exosomes were separated from free dye using the Total Exosome Isolation kit (#4478359, Invitrogen, Carlsbad, CA).

**In utero ultrasound-guided microinjection.** E8.0 pregnant dams were anesthetized by 3% isoflurane (Vetone, Boise, ID) in 100% oxygen initially, followed by 2% isoflurane during the rest of the procedure. The dams were placed supine on a mouse handling table where the integrated warmer of the heating platform set to 37 °C and a rectal thermometer was put in place to monitor body temperature. The dams' eyes were covered with a lubricant to prevent drying of the sclera. Abdomen hairs of the dams were removed. A 2-cm ventral midline incision was made approximately 1 cm above the vagina to open the abdomen and peritoneum. The number of embryos was counted to ensure adequate record keeping of which embryos were injected. To stabilize the uterus, a modified Petri dish with a 3-cm hole cut into the middle covered by a thin silicone membrane with a small slit cut in the center was placed over the dams' abdomens. The uterine horns were gently pulled up through the silicon membrane of the dish, which contained 0.9% saline to prevent dehydration. Under ultrasound (Vevo 770, VisualSonics, Canada) guidance, the uterus was penetrated by a microinjection needle (#C060609, Cooper-surgical) to reach the amniotic cavity. A total of 5 × 10<sup>9</sup> exosomes suspended in 280 nl of PBS were injected into the amniotic cavity. Following one injection, the handling table was repositioned to image and inject the next embryo. After injecting the desired number of embryos, the uterine horns were placed back into the abdomen. The maternal abdomen was sutured closed.

**Immunoblotting.** Immunoblotting was performed as described by Yang et al.<sup>8</sup>. Lysis buffer (Cell Signaling Technology, Danvers, MA) containing a protease inhibitor cocktail (Sigma, St. Louis, MO) was used to extract protein. Equal amounts of protein and Precision Plus Protein Standards (Bio-Rad, Hercules, CA) were resolved by SDS-PAGE and transferred onto Immobilon-P membranes (Millipore, Billerica, MA). Membranes were incubated in 5% nonfat milk for 45 min at room temperature, and then were incubated for 18 h at 4 °C with the following primary antibodies at dilutions of 1:1000 in 5% nonfat milk: FGF2, phosphorylated (p-)FGFR, p-AKT, BMP4, m-VEGFR1, p-VEGFR2, p-PERK, p-IRE1α, p-eIF2α, CHOP, caspase 8 and caspase 3. Following primary antibody incubation, membranes were washed with PBS and then exposed to HRP-conjugated related secondary antibodies at dilution of 1:10000. Signals were detected using the SuperSignal West Femto Maximum Sensitivity Substrate kit (Thermo Fisher Scientific, Waltham, MA). To ensure that equivalent amounts of protein were loaded on the SDS-PAGE gel, membranes were stripped and incubated with a mouse antibody against β-actin (Abcam, Cambridge, MA). All experiments were repeated in triplicate with the use of independently prepared tissue lysates. The detailed antibody information is provided in Supplementary Table 5, and whole Western blots are shown in Supplementary Fig. 9.

**Real-time PCR (RT-PCR).** mRNA was isolated from embryos using the Rneasy Mini kit (Qiagen, Hilden, Germany), and then reversely transcribed using the high-capacity cDNA archive kit (Applied Biosystem, Grand Island, NY). Real time-PCR for *Fgf2*, *Egfr*, *Bmp4*, *Vegfr2*, *mVegfr1*, *Calnexin*, *GRP94*, *PDIA*, *BiP*, *IRE1α*, *CHOP*, *Survivin*, and  $\beta$ -actin were performed using the Maxima SYBR Green/ROX qPCR Master Mix assay (Thermo Fisher Scientific, Waltham, MA) in the Step One Plus system (Applied Biosystem, Grand Island, NY). All primer sequences were listed in Supplementary Table 6.

**Tissue section staining.** Nondiabetic wild-type (WT), nondiabetic Tg, diabetic WT and diabetic Tg embryos were collected for a morphological examination at E10.5 and fixed in methacarn (methanol, 60%; chloroform, 30%; and glacial acetic acid, 10%). Embryos were dehydrated in alcohol and embedded in paraffin. And cut into 5- $\mu$ m sections. After deparaffinization and rehydration, and then stained with hematoxylin and eosin (H&E) and imaged under a Nikon Ni-U microscope (Nikon, Tokyo, Japan).

**Blood island quantification.** Five micrometer cross (vertical) sections of E8.5 conceptuses were stained by H&E. Yolk sac blood islands were counted and expressed against the yolk sac circumference. The yolk sac in an E8.5 conceptus cross-section is near-circular, so it was assumed to be a circle for calculating circumference. Ten sections of each conceptus were used and the data were averaged. Five conceptuses from different pregnant dams in each group were used to determine the numbers of blood islands in yolk sacs.

**Blood vessel density measurement.** E9.5 conceptuses were fixed with 4% paraformaldehyde in PBS overnight at 4 °C. For immunostaining analyses, controls were processed by omitting the primary antibody. The rat anti-mouse PECAM-1 antibody at a dilution of 1:200 (Abcam, Cambridge, MA) was used to stain the whole conceptuses. Samples were incubated in ABC solution (elite ABC kit, Vector Laboratories) for 30 min and then with the stable diaminobenzidine substrate solution (Vector Laboratories, Burlingame, CA). Yolk sacs were removed from the conceptuses and mounted on positively charged slides. Embryos were examined directly. PECAM-1 positive structures (vessel area) in the yolk sac and embryo were determined by capturing images and analyzing the PECAM-1-stained areas with the NIH ImageJ software (Version 1.62, National Institutes of Health, Bethesda, MD) by setting a consistent threshold for all slides. The PECAM-1-positive area was expressed as pixels-squared per high-power field.

**Dihydroethidium (DHE) staining.** DHE staining was used for immunofluorescent detection of superoxide. DHE reacts with superoxide that binds to cellular components such as protein and DNA, and manifested with bright red fluorescence. E8.5 embryos were fixed in 4% Paraformaldehyde (PFA) (Thermo Fisher Scientific, Waltham, MA) for 30 min, washed for 5 min each for three times with PBS, and then embedded in optimal cutting temperature compound (OCT) (Sakura Finetek, Torrance, CA). 10- $\mu$ m frozen embryonic sections were incubated with 1.5  $\mu$ M DHE for 5 min at room temperature and then washed for 3 times with PBS. Sections were counterstained with DAPI and mounted with aqueous mounting medium (Sigma, St. Louis, MO).

**Lipid hydroperoxide (LPO) quantification.** The degree of lipid peroxidation, an index of oxidative stress, was quantitatively assessed by the LPO assay by using the Calbiochem Lipid Hydroperoxide assay kit (Millipore, Bedford, MA) following the manufacture's manual. Briefly, E8.5 embryos were homogenized in HPLC-grade water (Thermo Fisher Scientific, Waltham, MA). The lipid hydroperoxides of each embryo tissue were extracted by degassed chloroform, and then measured by the absorbance of 500 nm after reaction with chromogen. The results were expressed as  $\mu$ M lipid hydroperoxides per microgram protein. Protein concentrations were assessed by the BioRad DC protein assay kit (BioRad, Hercules, CA).

**Detection of XBPI mRNA splicing.** mRNA was extracted from E8.5 embryos and reverse-transcribed to cDNA using the QuantiTect Reverse Transcription Kit (Qiagen, Hilden, Germany). The PCR primers for XBPI were as follows: forward, 5'-GAAGCGGAGCTAAGAACACG-3' and reverse, 5'-AGGCAACAGTGTCAGAGTCC-3'. If no XBPI mRNA splicing occurred, a 205 bp band was produced. When XBPI splicing occurred, a 205 bp band and a 179 bp main band were produced.

**TUNEL assay.** TUNEL assay was performed using the ApopTag Fluorescein in Situ Apoptosis Detection kit (# S7165, Millipore, Billerica, MA) as previously described<sup>8</sup>. Briefly, 5- $\mu$ m frozen embryonic sections were fixed with 4% PFA in PBS and incubated with TUNEL reaction agents. Three embryos from three different dams ( $n = 3$ ) in each group were used, and three sections per embryo were examined. TUNEL-positive cells in an area (about 200 cells) of the neuroepithelium were counted. The percentage of TUNEL-positive cells was calculated as a fraction of the total cell number, multiplied by 100 and averaged within the sections of each embryo.

**Statistics and reproducibility.** Data were presented as means  $\pm$  standard errors (SE). In animal studies, experiments were repeated at least three times, and embryonic samples from each replicate were from different dams. Statistical differences were determined by one-way analysis of variance (ANOVA) using the SigmaPlot 12.5 (SigmaStat, San Jose, CA). In one-way ANOVA analysis, Tukey test was used to estimate the significance of the results ( $P < 0.05$ ). The Chi square test and Fisher Exact test were used to estimate the significance of NTD incidence.

**Reporting summary.** Further information on research design is available in the Nature Research Reporting Summary linked to this article.

## Data availability

The datasets generated during and/or analyzed during the current study are available in the figshare repository<sup>63</sup>.

Received: 12 October 2020; Accepted: 21 June 2022;

Published online: 01 July 2022

## References

- Mathews, T. J. & Driscoll, A. J. Trends in Infant Mortality in the United States, 2005–2014. *NCHS Data Brief* **265**, 1–8 (2017).
- McGough, I. J. & Vincent, J. P. Exosomes in developmental signalling. *Development* **143**, 2487–2493 (2016).
- Saha, P. et al. Circulating exosomes derived from transplanted progenitor cells aid the functional recovery of ischemic myocardium. *Sci. Transl. Med.* **11**, <https://doi.org/10.1126/scitranslmed.aau1168> (2019).
- Wheatley, S. J. & Anderi, D. C. Survivin at a glance. *J. Cell Sci.* **132**, <https://doi.org/10.1242/jcs.223826> (2019).
- Khan, S. et al. Survivin is released from cancer cells via exosomes. *Apoptosis: J. Program. Cell Death* **16**, 1–12 (2011).
- Shibuya, F. et al. Failure of blood-island formation and vasculogenesis in Flk-1-deficient mice. *Nature* **376**, 62–66 (1995).
- Zyberts, F. et al. Lack of endothelial cell survivin causes embryonic defects in angiogenesis, cardiogenesis, and neural tube closure. *Blood* **109**, 4742–4752 (2007).
- Yang, P. et al. Maternal hyperglycemia activates an ASK1-FoxO3a-caspase 8 pathway that leads to embryonic neural tube defects. *Sci. Signal.* **6**, ra74 (2013).
- Wang, F. et al. Ask1 gene deletion blocks maternal diabetes-induced endoplasmic reticulum stress in the developing embryo by disrupting the unfolded protein response signalosome. *Diabetes* **64**, 973–988 (2015).
- Wang, F. et al. Protein kinase C- $\alpha$  suppresses autophagy and induces neural tube defects via miR-129-2 in diabetic pregnancy. *Nat. Commun.* **8**, 15182 (2017).
- Yang, P. et al. Tip60- and sirtuin 2-regulated MARCKS acetylation and phosphorylation are required for diabetic embryopathy. *Nat. Commun.* **10**, 282 (2019).
- Pavlinkova, G., Salbaum, J. M. & Kappen, C. Maternal diabetes alters transcriptional programs in the developing embryo. *BMC Genomics* **10**, 274 (2009).
- Wentzel, P., Gareskog, M. & Eriksson, U. J. Decreased cardiac glutathione peroxidase levels and enhanced mandibular apoptosis in malformed embryos of diabetic rats. *Diabetes* **57**, 3344–3352 (2008).
- Wallingford, J. B., Niswander, L. A., Shaw, G. M. & Finnell, R. H. The continuing challenge of understanding, preventing, and treating neural tube defects. *Science* **339**, 1222002 (2013).
- Correa, A. et al. Diabetes mellitus and birth defects. *Am. J. Obstet. Gynecol.* **199**, e231–e237 (2008).
- Greene, M. F., Hare, J. W., Cloherty, J. P., Benacerraf, B. R. & Soeldner, J. S. First-trimester hemoglobin A1 and risk for major malformation and spontaneous abortion in diabetic pregnancy. *Teratology* **39**, 225–231 (1989).
- Lucas, M. J., Leveno, K. J., Williams, M. L., Raskin, P. & Whalley, P. J. Early pregnancy glycosylated hemoglobin, severity of diabetes, and fetal malformations. *Am. J. Obstet. Gynecol.* **161**, 426–431 (1989).
- Suhonen, L., Hiilesmaa, V. & Teramo, K. Glycaemic control during early pregnancy and fetal malformations in women with type I diabetes mellitus. *Diabetologia* **43**, 79–82 (2000).
- Wang, F., Fisher, S. A., Zhong, J., Wu, Y. & Yang, P. Superoxide dismutase 1 in vivo ameliorates maternal diabetes mellitus-induced apoptosis and heart defects through restoration of impaired wnt signaling. *Circulation. Cardiovascular Genet.* **8**, 665–676 (2015).
- Yang, P. & Reece, E. A. Role of HIF-1 $\alpha$  in maternal hyperglycemia-induced embryonic vasculopathy. *Am. J. Obstet. Gynecol.* **204**, e331–e332 (2011).



21. Fine, E. L., Horal, M., Chang, T. I., Fortin, G. & Loeken, M. R. Evidence that elevated glucose causes altered gene expression, apoptosis, and neural tube defects in a mouse model of diabetic pregnancy. *Diabetes* **48**, 2454–2462 (1999).
22. Salbaum, J. M. & Kappen, C. Neural tube defect genes and maternal diabetes during pregnancy. *Birth Defects Res. A Clin. Mol. Teratol.* **88**, 601–611 (2010).
23. Berdahl, D. M., Blaine, J., Van Voorhis, B. & Dokras, A. Detection of enlarged yolk sac on early ultrasound is associated with adverse pregnancy outcomes. *Fertil. Steril.* **94**, 1535–1537 (2010).
24. Yang, P., Zhao, Z. & Reece, E. A. Blockade of c-Jun N-terminal kinase activation abrogates hyperglycemia-induced yolk sac vasculopathy in vitro. *Am. J. Obstet. Gynecol.* **198**, 321 e321–321 e327 (2008).
25. Kodet, O. et al. Melanoma cells influence the differentiation pattern of human epidermal keratinocytes. *Mol. Cancer* **14**, 1 (2015).
26. Yang, P., Zhao, Z. & Reece, E. A. Activation of oxidative stress signaling that is implicated in apoptosis with a mouse model of diabetic embryopathy. *Am. J. Obstet. Gynecol.* **198**, 130 e131–130 e137 (2008).
27. Doetschman, T., Shull, M., Kier, A. & Coffin, J. D. Embryonic stem cell model systems for vascular morphogenesis and cardiac disorders. *Hypertension* **22**, 618–629 (1993).
28. Kessler, D. S. & Melton, D. A. Vertebrate embryonic induction: mesodermal and neural patterning. *Science* **266**, 596–604 (1994).
29. Zhong, J., Xu, C., Reece, E. A. & Yang, P. The green tea polyphenol EGCG alleviates maternal diabetes-induced neural tube defects by inhibiting DNA hypermethylation. *Am. J. Obstet. Gynecol.* **215**, 368 e361–368 e310 (2016).
30. Wei, D. & Loeken, M. R. Increased DNA methyltransferase 3b (Dnmt3b)-mediated CpG island methylation stimulated by oxidative stress inhibits expression of a gene required for neural tube and neural crest development in diabetic pregnancy. *Diabetes* **63**, 3512–3522 (2014).
31. Yu, J., Wu, Y. & Yang, P. High glucose-induced oxidative stress represses sirtuin deacetylase expression and increases histone acetylation leading to neural tube defects. *J. Neurochem* **137**, 371–383 (2016).
32. Yang, P. & Li, H. Epigallocatechin-3-gallate ameliorates hyperglycemia-induced embryonic vasculopathy and malformation by inhibition of Foxo3a activation. *Am. J. Obstet. Gynecol.* **203**, 75 e71–75 e76 (2010).
33. Poole, T. J., Finkelstein, E. B. & Cox, C. M. The role of FGF and VEGF in angioblast induction and migration during vascular development. *Developmental Dyn.* **220**, 1–17 (2001).
34. Flamme, I. & Risau, W. Induction of vasculogenesis and hematopoiesis in vitro. *Development* **116**, 435–439 (1992).
35. Brueckner, B. et al. Epigenetic reactivation of tumor suppressor genes by a novel small-molecule inhibitor of human DNA methyltransferases. *Cancer Res.* **65**, 6305–6311 (2005).
36. Li, X., Xu, C. & Yang, P. c-Jun NH2-terminal kinase 1/2 and endoplasmic reticulum stress as interdependent and reciprocal causative in diabetic embryopathy. *Diabetes* **62**, 599–608 (2013).
37. Wang, F., Reece, E. A. & Yang, P. Superoxide dismutase 1 overexpression in mice abolishes maternal diabetes-induced endoplasmic reticulum stress in diabetic embryopathy. *Am. J. Obstet. Gynecol.* **209**, 335 e341–335 e347 (2013).
38. Ambrosini, G., Adida, C. & Altieri, D. C. A novel anti-apoptosis gene, survivin, expressed in cancer and lymphoma. *Nat. Med.* **3**, 917–921 (1997).
39. Dohi, T., Beltrami, E., Wall, N. R., Plescia, J. & DeCruz, D. C. Mitochondrial survivin inhibits apoptosis and promotes tumorigenesis. *J. Clin. Investig.* **114**, 1117–1127 (2004).
40. Tkach, M. & Thery, C. Communication by extracellular vesicles: where we are and where we need to go. *Cell* **148**, 1228–1232 (2016).
41. Seo, N. et al. Activated CD8(+) T cell extracellular vesicles prevent tumour progression by targeting of lesional mesenchymal cells. *Nat. Commun.* **9**, 435 (2018).
42. Zhou, M. et al. Fibroblast growth factor 2 control of vascular tone. *Nat. Med.* **4**, 201–207 (1998).
43. Zhao, Z., Yang, P., Eckert, R. L. & Reece, E. A. Caspase-8: a key role in the pathogenesis of diabetic embryopathy. *Birth Defects Res. B Dev. Reprod. Toxicol.* **85**, 72–77 (2009).
44. Hoshino, T., Kuznetsov, A. V., Obexer, P. & Ausserlechner, M. J. BIRC5/Survivin enhances aerobic glycolysis and drug resistance by altered regulation of the mitochondrial fusion/fission machinery. *Oncogene* **32**, 4748–4757 (2013).
45. Hoffman, W. H., Biade, S., Zilfou, J. T., Chen, J. & Murphy, M. Transcriptional repression of the anti-apoptotic survivin gene by wild type p53. *J. Biol. Chem.* **277**, 3247–3257 (2002).
46. Gareskog, M., Cederberg, J., Eriksson, U. J. & Wentzel, P. Maternal diabetes in vivo and high glucose concentration in vitro increases apoptosis in rat embryos. *Reprod. Toxicol.* **23**, 63–74 (2007).
47. Pani, L., Horal, M. & Loeken, M. R. Rescue of neural tube defects in Pax-3-deficient embryos by p53 loss of function: implications for Pax-3-dependent development and tumorigenesis. *Genes Dev.* **16**, 676–680 (2002).
48. Srivastava, A. et al. Exploitation of exosomes as nanocarriers for gene-, chemo-, and immune-therapy of cancer. *J. Biomed. Nanotechnol.* **12**, 1159–1173 (2016).
49. Rana, S., Yue, S., Stadel, D. & Zoller, M. Toward tailored exosomes: the exosomal tetraspanin web contributes to target cell selection. *Int. J. Biochem. Cell Biol.* **44**, 1574–1584 (2012).
50. Dong, D. et al. New development of the yolk sac theory in diabetic embryopathy: molecular mechanism and link to structural birth defects. *Am. J. Obstet. Gynecol.* **214**, 192–202 (2016).
51. Xu, C. et al. Maternal diabetes induces senescence and neural tube defects sensitive to the senomorphic rapamycin. *Sci. Adv.* **7**, eabf5089 (2021).
52. Cao, S., Shen, W. B., Reece, E. A. & Yang, P. Deficiency of the oxidative stress-responsive kinase p70S6K1 restores autophagy and ameliorates neural tube defects in diabetic embryopathy. *Am. J. Obstetrics Gynecol.*, <https://doi.org/10.1016/j.ajog.2020.05.015> (2020).
53. Cao, S., Reece, E. A., Shen, W. B. & Yang, P. Restoring BMP4 expression in vascular endothelial progenitors ameliorates maternal diabetes-induced apoptosis and neural tube defects. *Cell Death Dis.* **11**, 859 (2020).
54. Kamimoto, Y. et al. Transgenic mice overproducing human thioredoxin-1, an antioxidative and anti-apoptotic protein, prevent diabetic embryopathy. *Diabetologia* **53**, 2046–2055 (2010).
55. Xu, C., Chen, X., Reece, E. A., Lu, W. & Yang, P. The increased activity of a transcription factor inhibits autophagy in diabetic embryopathy. *Am. J. Obstet. Gynecol.* **220**, 108 e101–108 e112 (2019).
56. Sugimura, Y. et al. Prevention of neural tube defects by loss of function of inducible nitric oxide synthase in mice: a mouse model of streptozotocin-induced diabetes. *Diabetologia* **52**, 962–971 (2009).
57. Gabbay-Benziv, R., Reece, E. A., Wang, F. & Yang, P. Birth defects in pregestational diabetes: Defect range, glycemic threshold and pathogenesis. *World J. Diabetes* **6**, 481–488 (2015).
58. Reece, E. A., Witztum, A., Homko, C. J., Hagay, Z. & Wu, Y. K. Synchronization of the factors critical for diabetic teratogenesis: an in vitro model. *Am. J. Obstet. Gynecol.* **174**, 1284–1288 (1996).
59. Miller, J. L. et al. First trimester detection of fetal anomalies in pregestational diabetes: nuchal translucency, ductus venosus Doppler, and maternal glycosylated hemoglobin. *Am. J. Obstet. Gynecol.* **208**, 385 e381–385 e388 (2013).
60. Ronicke, W., Risau, W. & Breier, G. Characterization of the endothelium-specific murine vascular endothelial growth factor receptor-2 (Flk-1) promoter. *Circulation Res.* **79**, 277–285 (1996).
61. Xu, C., Li, X., Wang, F., Weng, H. & Yang, P. Trehalose prevents neural tube defects by correcting maternal diabetes-suppressed autophagy and neurogenesis. *Am. J. Physiol. Endocrinol. Metab.* **305**, E667–E678 (2013).
62. Li, X., Weng, H., Xu, C., Reece, E. A. & Yang, P. Oxidative stress-induced JNK1/2 activation triggers proapoptotic signaling and apoptosis that leads to diabetic embryopathy. *Diabetes* **61**, 2084–2092 (2012).
63. Yang, P. et al. Functional cargos of exosomes derived from Flk-1+ vascular progenitors enable neurulation and ameliorate embryonic anomalies in diabetic pregnancy. *figshare*, <https://doi.org/10.6084/m9.figshare.19694479.v1> (2022).

## Acknowledgements

The authors thank the Office of Dietary Supplements at the NIH. We thank Hua Li for her technical support and Dr. Julie Rosen at the University of Maryland School of Medicine for critical reviewing. This study is supported by National Institutes of Health (NIH) grants R01 HL131737, R01HD100195, R01HD102206, R01DK083243, R01DK101972, and R01DK103024 and an American Diabetes Association Basic Science Award (1-13-BB-2520).

## Author contributions

S.C., Y.W., C.X., and W.-B.S. researched the data. E.A.R. and S.K. analyzed the data and revised the manuscript. P.Y. conceived the project, designed the experiments, and wrote the manuscript. All authors approved the final version of the paper.

## Competing interests

The authors declare no competing interests.

## Additional information

**Supplementary information** The online version contains supplementary material available at <https://doi.org/10.1038/s42003-022-03614-3>.

**Correspondence** and requests for materials should be addressed to Peixin Yang.

**Peer review information** *Communications Biology* thanks the anonymous reviewers for their contribution to the peer review of this work. Primary Handling Editors: Karli Montague-Cardoso and Christina Karlsson Rosenthal. Peer reviewer reports are available.

**Reprints and permission information** is available at <http://www.nature.com/reprints>

**Publisher's note** Springer Nature remains neutral with regard to jurisdictional claims in published maps and institutional affiliations.



**Open Access** This article is licensed under a Creative Commons Attribution 4.0 International License, which permits use, sharing, adaptation, distribution and reproduction in any medium or format, as long as you give appropriate credit to the original author(s) and the source, provide a link to the Creative Commons license, and indicate if changes were made. The images or other third party material in this article are included in the article's Creative Commons license, unless indicated otherwise in a credit line to the material. If material is not included in the article's Creative Commons license and your intended use is not permitted by statutory regulation or exceeds the permitted use, you will need to obtain permission directly from the copyright holder. To view a copy of this license, visit <http://creativecommons.org/licenses/by/4.0/>.

© The Author(s) 2022

RETRACTED ARTICLE